Pharmaceutical Research, Vol. 24, No. 10, October 2007 (© 2007)
DOI: 10.1007/s11095-007-9309-1

Featured Article

Histamine-induced Myosin Light Chain Phosphorylation Breaks Down the Barrier Integrity of Cultured Corneal Epithelial Cells

Ying Guo,[1] Charanya Ramachandran,[1] Minati Satpathy,[1] and Sangly P. Srinivas[1,2]

Received July 11, 2006; accepted April 2, 2007; published online May 4, 2007

Purpose. To investigate changes in the phosphorylation of myosin light chain (MLC) in response to histamine and its effect on the barrier integrity of corneal epithelial cells.
Materials and Methods. Experiments were performed in bovine corneal epithelial cells (BCEC). RT-PCR and Western blotting were employed to characterize expression of H1 receptors and MLC kinase (MLCK). Phosphorylation of MLC was assessed by urea-glycerol gel electrophoresis and Western blotting. Barrier integrity was determined as permeability to horseradish peroxidase (HRP; 44 kDa) across monolayers grown on porous filters.
Results. Expression of both H1 receptors and MLCK was found in BCEC. Exposure to histamine induced significant MLC phosphorylation concomitant with an increase in HRP permeability. In addition, organization of the cortical actin found in resting cells was disrupted. In contrast to histamine, ATP (a P2Y receptor agonist) induced dephosphorylation of MLC. Pre-exposure to ATP reduced the effect of histamine on HRP permeability and disruption of cortical actin.
Conclusion. MLC phosphorylation, a biochemical pre-requisite for increased contractility of the actin cytoskeleton, led to histamine-induced breakdown of the barrier integrity in the corneal epithelial cells. This is attributed to weakening of the tethering forces at the tight junctions by the centripetal forces produced by increased actin contractility.

KEY WORDS: actin cytoskeleton; corneal epithelium; myosin light chain; paracellular permeability.

INTRODUCTION

The stratified corneal epithelium forms a barrier on the ocular surface, protecting the interior of the eye from invasion by pathogens, fluid, and noxious agents. It also limits the intraocular bioavailability of most topical ophthalmic drugs. This barrier function of the corneal epithelium depends on tight junctions located in its superficial squamous cell layers (1,2). The tight junctions seal the intercellular spaces and, thereby promote the barrier property of epithelia (3,4). They also help to maintain polarity of the cells by restricting diffusion of membrane proteins between the apical and basolateral membranes (3,4). The proteins that constitute the tight junctional complex include the trans-membrane molecules occludin, claudin, and junctional adhesion molecule (JAM). In addition, several membrane-associated cytoplasmic proteins such as zonula occluden proteins (ZO-1, ZO-2, and ZO-3) form linker molecules attaching the tight junctional molecules to the actin cytoskeleton. The barrier property conferred by the tight junctions is dynamic, and is frequently altered by various physiological and pathological stimuli (5–9). However, the molecular mechanisms underlying the regulation are poorly understood.

Actin cytoskeleton, which is linked to the tight junctional complex (10), is implicated in regulation of the barrier integrity (11–14). Enhanced contractility of the actin cytoskeleton is known to induce hyperpermeability in several endothelial (15,16) and epithelial (17,18) cell types. Usually, the actin cytoskeleton is densely organized in the cortical region into a thick belt, named the peri-junctional actomyosin ring (PAMR) (13). A centripetal force, generated in response to increased contractility of the PAMR, opposes tethering forces at the sites of cell–cell adherence (12–14). The tethering forces are essential for trans-membrane interactions of the tight junctional proteins between two apposing cells. Therefore, a weakening of tethering forces breaks down the barrier integrity of the epithelium (13).

The contractility of actin cytoskeleton is regulated by phosphorylation of the myosin light chain (MLC), which triggers actomyosin interaction. This induces centripetal forces that can disrupt the tight junctions. Increased MLC phosphorylation is also known to cause redistribution of occludin and ZO-1 at the tight junctions, which can contribute to a loss of

[1] School of Optometry, Indiana University, 800 East Atwater Avenue, Bloomington, Indiana 47405, USA.
[2] To whom correspondence should be addressed. (e-mail: srinivas@indiana.edu)

barrier integrity (19). The status of MLC phosphorylation is a balance between two opposing pathways: phosphorylation mediated by MLC kinase (MLCK) and dephosphorylation by MLC phosphatase (MLCP) (20,21). MLCK is activated by binding to Ca^{2+}-calmodulin complex. In contrast to this Ca^{2+}-sensitive mechanism, MLC phosphorylation is modulated by Rho kinase and PKC through inhibition of the activity of MLCP (20,21). Thus, many G-protein coupled receptors (GPCRs), known to elevate $[Ca^{2+}]_i$ and activate PKC or RhoA (a small GTPase which activates Rho kinase), affect the actin contractility through MLC phosphorylation (20,21).

Inflammatory mediators, such as thrombin and histamine, have been shown to break down the tight junctions through specific G protein coupled receptors (GPCRs) in vascular (22,23) and corneal (16,24) endothelial cells by inducing MLC phosphorylation. Histamine levels, which are usually low in tears, are greatly increased during allergy and inflammation (25,26). In this study, we have investigated MLC phosphorylation in bovine corneal epithelial cells (BCEC) in response to histamine to examine the effect of actin contractility on barrier integrity. We have also employed ATP to induce dephosphorylation of MLC (27,28).

MATERIALS AND METHODS

Bovine Corneal Epithelial Cell Culture

Bovine eyes delivered on ice from a local slaughterhouse were disinfected with 1% iodine. Corneal epithelium, along with a small thickness of stroma, was dissected and incubated in 2 U/ml dispase at 37°C for 90 min. Sheets of the epithelium were then removed under a dissection microscope and incubated further at 37°C in 0.05% trypsin. After 15 min, trypsin was deactivated by adding a serum-containing growth medium and cells were collected by centrifugation. Cells were then cultured in a DMEM/F12 (GIBCO BRL, Grand Island, NY) culture medium supplemented with 10% bovine calf serum, 5 μg/ml insulin, 5 ng/ml epidermal growth factor (Invitrogen, Grand Island, NY), and an antibiotic-antimycotic mixture (50 μg/ml gentamicin and 50 ng/ml amphotericin B) at 37°C in a humidified atmosphere containing 5% CO_2 and 95% air. Although there is a slight possibility for fibroblast contamination from the stroma, the epithelial characteristics was confirmed at a molecular level by immunofluorescence labeling of keratin-3 (monoclonal anti-epithelial keratin-3 antibody, MP Biomedicals, Aurora, Ohio), an intermediate filament that is specific to corneal epithelium. This also excludes contamination with corneal endothelial cells which were not disturbed during epithelial peeling due to protection of stroma. The second and third passage cells were used for all experiments.

RT-PCR Assay

Total RNA was isolated from BCEC using Trizol® reagent (GIBCO BRL, Grand Island, NY) and quantified by absorption at 260 nm. First-strand cDNA was synthesized using the SuperScript III Reverse Transcriptase (Invitrogen, Grand Island, NY). PCR was performed for 35 cycles and the products were run on a 1.5% agarose gel and visualized by ethidium bromide staining along with 100/1,000 bp markers (Amersham Biosciences, Piscataway, NJ). All primers employed in this study (Table I) have been tested with bovine corneal endothelial cells as positive control.

Table I. Primers Used in RT-PCR Assays

Gene	Accession No.	Primer	Sequence (5′–3′)	Homology	Size
H1R	BC060802	F	TCATGCTCTGGTTCTATGCCAAG	Bovine	758
		R	AGCCCAGCCAGATGGTGAACATG		
P2Y1	X87628	F	TCCCTAGGGAAAGCGCAGTC	Bovine	561
		R	GAACATCCAGATGGCCACGC		
P2Y2	AF005153	F	CCCCTGTGCTGTACTTCGTCAC	Bovine	274
		R	GCAGAGGACGAAGACAGTCAGC		
A2A	AY136748	F	AACCTGCAGAACGTCACCAACT	Human/Canine	789
		R	GGAAGGTCTGGCGGAACTC		
A2B	NM_053294	F	GCTCCATCTTCAGCCTTCTG	Human/Canine	438
		R	AGTGACTTGGCTGCATGGATCT		
CD39	AF005940	F	GAAGGTGCCTATGGCTGGATTAC	Human/Rat/Mouse	870
		R	TGTTGGTCAGGTTCAGCATGTAG	Human/Rat/Mouse	
CD73	AF034840	F	AGTACCAGGGCACCATCTGGTTC	Human/Rat/Mouse	1,317
		R	ATATCTTGGTCACCAGAGTCATG	Human/Rat/Mouse	
MLCK	XM_590786	F	CAGAAAACGGGCAATGCTGTGA	Bovine	246
		R	TCTAGCAGCACTTCCCTCCACA		
EC-MLCK	HSU48959	F	GCTTGGTCAGCCTGTTGTTTCCAA	Human	159
		R	TTGCAGGAGAATCGTCCCATCTGT		
SM-MLCK	S571131	F	GCCTTCAAGCAGAAGCTGCAAGAT	Bovine	111
		R	TCCATTCAGCGTCCAGATGATGGT		

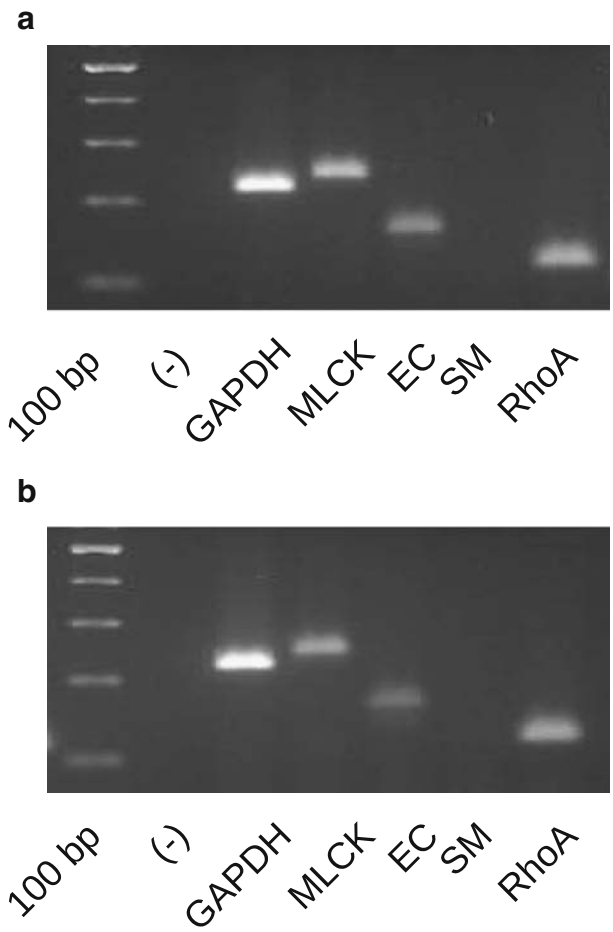

Fig. 1. Expression of MLCK and RhoA in BCEC. **a** In cultured BCEC, RT-PCR showed positive bands for both MLCK (246 bp) and RhoA (117 bp). The EC-MLCK isoform was found at the expected band size of 159 bp, while the transcript for SM-MLCK was absent (expected size: 185 bp). GAPDH (226 bp) was employed as the housekeeping gene. **b** Fresh cell scrapings from bovine corneal epithelium showed a comparable expression level of both MLCK and RhoA. No positive band was found for SM-MLCK. (−): negative control; EC: EC-MLCK; SM: SM-MLCK.

Expression of H1 Receptors

A purified polyclonal antibody (Rabbit anti-histamine receptor1; 1:1,000 dilution; Chemicon International, Temecula, CA) known to recognize rat H1 receptors was used. Cells were lysed using an ice-cold lysis buffer containing 50 mM Tris HCl (pH 7.6), 150 mM NaCl, 1% Triton X-100, 2 mM EGTA (pH 8.0), EDTA, dithiothreitol, phenyl methyl sulphonyl fluoride (PMSF), NaF, and a protease inhibitor cocktail (Roche, Indianapolis). After a pre-clearing centrifugation step, the lysate was subjected to 10% SDS-PAGE and immunoblotting. Membranes were blocked with TBST (Tris-buffered saline with Tween 20) containing 5% nonfat dry milk for 1 h at room temperature, and subsequently incubated overnight at 4°C with the primary antibody diluted in 5% dry milk in TBST. The membranes were then washed thrice (15 min each) with TBST, and the blots were visualized using the peroxidase-conjugated secondary antibody and chemiluminescence kit.

Quantitative Estimation of MLC Phosphorylation

MLC phosphorylation was assayed using urea-glycerol gel electrophoresis followed by western blotting as described earlier (16,24,28,29). Cells were grown on 60 mm Petri dishes and serum-starved for 16–18 h before drug treatment. Protein extracts were dissolved in a urea sample buffer and subjected to electrophoresis for 3 h. The phosphorylated and non-phosphorylated MLC were detected by immunoblotting using a polyclonal anti-MLC antibody (E201; 1:3,000 dilution). The migration rates of the different forms of MLC are as follows: PP (di-phosphorylated form) > P (mono-phosphorylated form) >‘ NP (non-phosphorylated form). Blots were washed with TBST and visualized using the chemiluminescence kit. The intensities of the MLC bands in the blots were quantified using a custom-made software program. The

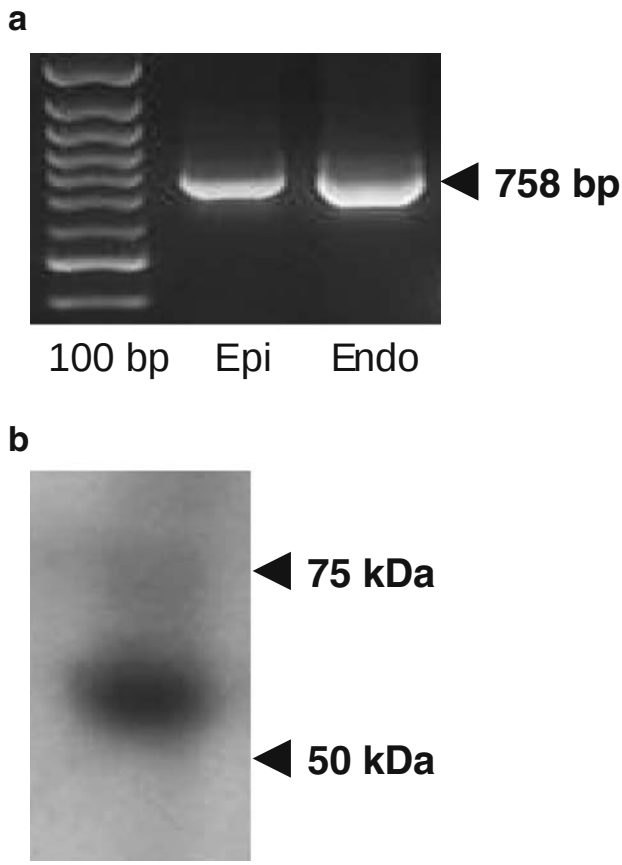

Fig. 2. Expression of the H1 receptor in BCEC. **a** RT-PCR results showed expression of the transcript for H1 receptor at the expected band size of 758 bp. Bovine corneal endothelial cell culture, which has been demonstrated to express H1 receptors, was used as a positive control. **b** Western blotting confirmed the expression of H1 receptors (55 kDa). Notes: *Epi*: epithelial cells; *Endo*: endothelial cells.

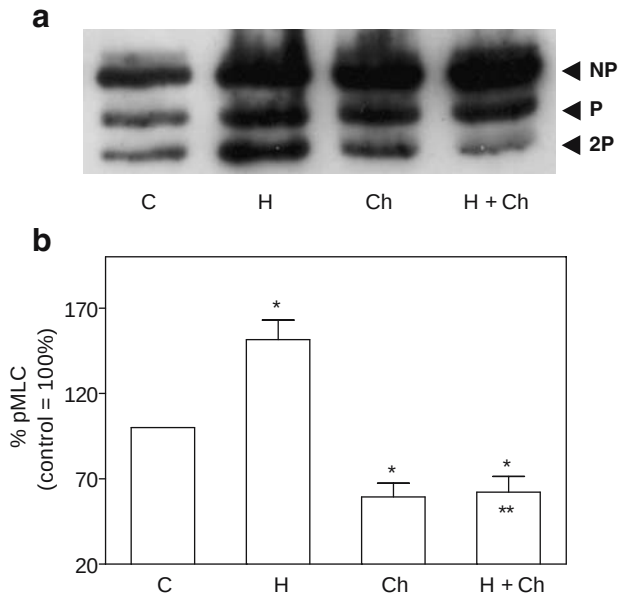

Fig. 3. Histamine-stimulated MLC phosphorylation was suppressed by chelerythrine. Cells were serum-starved for 16–18 h before exposure to histamine (100 μm, 2 min) or chelerythrine (10 μm, 10 min) or both. Extracted protein was subjected to urea-glycerol gel electrophoresis followed by Western blotting. **a** A representative urea-glycerol gel showing enhanced MLC phosphorylation in response to histamine (Lane: H) and inhibition of this response by chelerythrine (Lane: H + Ch). **b** A summary plot of densitometric analysis of the results. The fraction of the phosphorylated MLC (denoted by %pMLC) was calculated as the ratio of phosphorylated MLC (sum of P and PP) to the total MLC (sum of NP, P, and PP). Notes: *C*: control; *H*: histamine; *Ch*: chelerythrine. * Indicates significant difference from the control. C vs. H: $p<0.01$; C vs. Ch or H + Ch: $p<0.05$; ** Indicates significant difference H vs. H + Ch: $p<0.001$.

fraction of the phosphorylated MLC (denoted by % pMLC) was calculated as the ratio of phosphorylated MLC (sum of P and PP) to the total MLC (sum of NP, P, and PP).

HRP Assay of Barrier Integrity

Cells were grown to confluence on porous matrices (Transwell™, Costar, MA) before being exposed to drugs in the apical bath that also contained HRP (440 μg/ml; Sigma, St. Louis, MO). Samples from the basolateral chamber were analyzed for peroxidase activity using a spectrophotometric assay (15,16). The absorbance at 470 nm is proportional to the concentration of HRP that diffused into the basolateral chamber.

Staining of Actin Cytoskeleton

Cells grown on 12 mm glass coverslips were serum-starved and treated with desired drugs. After washing with PBS, cells were fixed for 10 min with 3.7% paraformaldehyde/ PBS and permealized for 5 min with 0.2% Triton X-100 (Sigma, St. Louis, MO). Cells were then incubated with Texas red phalloidin (Molecular Probes, Eugene, OR; 1:500) in dark for 45 min. Coverslips were mounted with an antifade agent (Molecular Probes, Eugene, OR) and viewed under a fluorescence microscope (Nikon, 60×1.2 NA; λ_{ex}=542 nm and λ_{em}=563 nm).

Drugs and Chemicals

Bovine calf serum was purchased from Hyclone (Logan, UT). All other cell culture supplies were from GIBCO BRL (Grand Island, NY). Enhanced chemiluminescence reagent

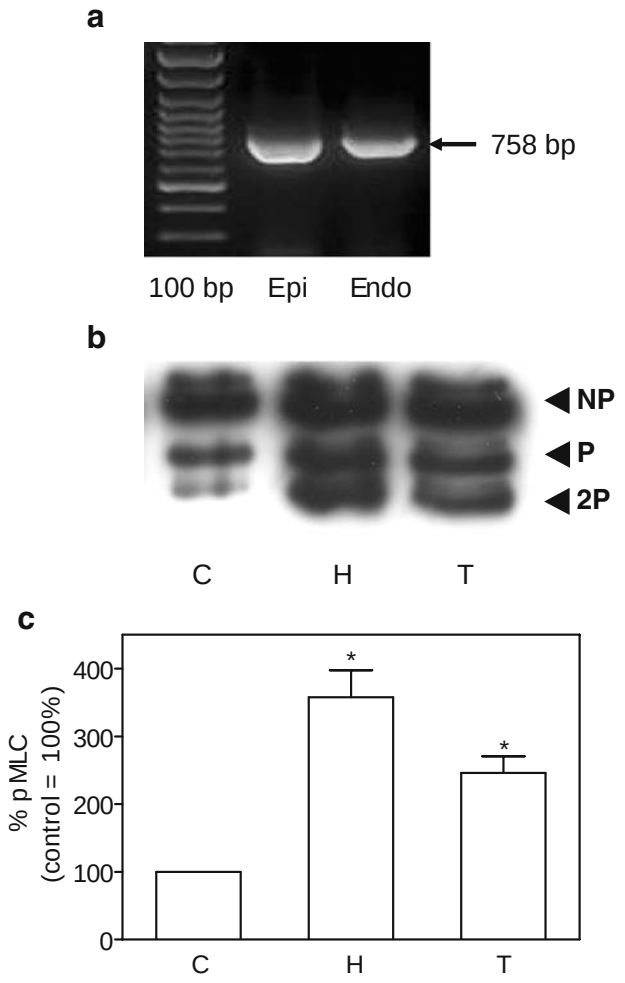

Fig. 4. Histamine stimulated MLC phosphorylation in freshly scraped BCEC. Cells were gently scraped off fresh bovine corneal epithelium and collected for RNA or protein extraction. **a** RT-PCR results indicate presence of the transcript for H1 receptors (758 bp) in the corneal epithelium. Bovine corneal endothelial cell culture was used as a positive control. **b** A representative urea-glycerol gel showing increased MLC phosphorylation with exposure to histamine (100 μm, 2 min; Lane: H). As a positive control, PAR-1 agonist thrombin (2 U/ml, 2 min) also caused significant MLC phosphorylation (Lane: T). **c** Summary of the densitometric analysis of the results. Notes: *Epi*: epithelial cells; *Endo*: endothelial cells; *C*: control; *H*: histamine; *T*: thrombin. * Indicates significant difference from the control. C vs. H: $p<0.01$; C vs. T: $p<0.05$.

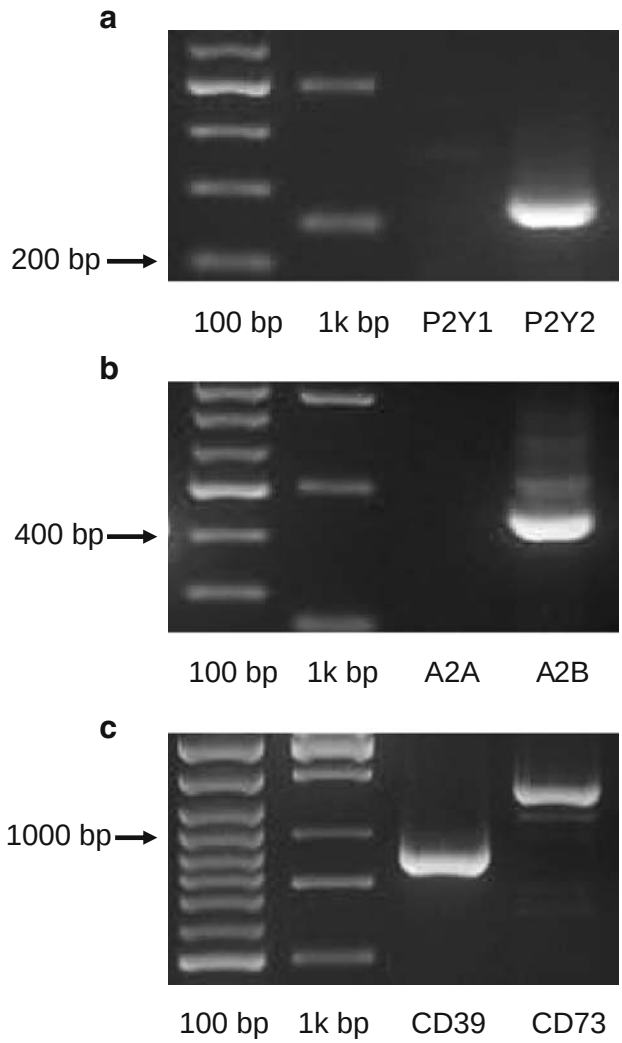

Fig. 5. Expression of P2Y2 and A2B adenosine receptors in cultured epithelial cells. Total RNA was extracted using Trizol® reagent and subjected to RT-PCR assay. **a** Expression of P2Y2 purinergic receptors was shown at the expected band size of 274 bp. No positive band was found for P2Y1 (expected size: 561 bp). **b** A positive band was found at 438 bp, indicating expression of adenosine receptor A2B at the mRNA level; expression of A2A was not detectable (expected size: 789 bp). **c** Positive bands corresponding to ecto-nucleotidases CD39 and CD73, which together catalyze ATP to adenosine, were found at 870 and 1,317 bp, respectively.

was purchased from Amersham-Pharmacia Biotech (Piscataway, NJ). Phalloidin conjugated to Texas red was obtained from Molecular Probes (Eugene, OR). All other drugs/reagents were purchased from Sigma (St. Louis, MO).

Statistical Analysis

Data was analyzed using one-way ANOVA with Bonferroni's post-test analysis (Prism 4.0 for Windows; GraphPad Software Inc., San Diego, CA). A value of $p<0.05$ was considered statistically significant.

RESULTS

Expression of MLCK Isoforms and RhoA

MLCK and RhoA are the two key regulators of MLC phosphorylation (20,21,30). MLCK has two isoforms transcribed from a single gene: SM-MLCK (the smooth muscle MLCK; 130 kDa), which is abundant in smooth muscles; and a higher molecular weight isoform EC-MLCK (the vascular endothelial MLCK; 210 kDa) (31). In addition to MLCK, RhoA also promotes MLC phosphorylation by inhibiting MLCP through its downstream effector Rho kinase (32). RT-PCR findings in Fig. 1a indicate expression of both MLCK and RhoA in BCEC with the positive bands corresponding to EC-MLCK and RhoA shown at 159 and 117 bp, respectively. No band was detected at the expected size (185 bp) for SM-MLCK. The identities of all PCR products were confirmed by sequencing. Comparable expression levels of both EC-MLCK and RhoA were found in the fresh corneal epithelial cells (Fig. 1b).

Expression of H1 Receptors

Expression of H1 receptors was examined at both the mRNA and protein levels. The RT-PCR results show a positive band at the expected size of 758 bp for H1 receptors (Fig. 2a). Cultured bovine corneal endothelial cells were used as a positive control. Results of the Western blotting are shown in Fig. 2b. The band at 55 kDa corresponds to the H1 receptor.

Effect of Histamine on MLC Phosphorylation

The activation of $G_{\alpha q/11}$ -coupled H1 receptors leads to Ca^{2+} mobilization (33–35), which can stimulate the Ca^{2+}-calmodulin-dependent MLCK (21,30). In addition, MLCP can be inhibited through PKC-dependent mechanisms (21,30). Thus, both mechanisms can lead to MLC phosphorylation. In BCEC, exposure to histamine (100 μm, 2 min) enhanced MLC phosphorylation by 51.5±11.5% (n=5, $p<0.01$) (Fig. 3). Chelerythrine (10 μm, 10 min), a selective PKC inhibitor, reduced the histamine-induced MLC phosphorylation to 62.1±9.3% (n=5, $p<0.001$) (Fig. 3b; Lane: H + Ch). Treatment with chelerythrine alone caused a 40.6% reduction in MLC phosphorylation compared to the control (n=5, $p<0.05$).

The above findings were confirmed in the fresh epithelial cells scraped from bovine cornea. As shown in Fig. 4a, transcript for the H1 receptor was found at the expected band size of 758 bp. In these cells, histamine (100 μm, 2 min) elicited a remarkable increase in MLC phosphorylation (357.8±39.8%; n=3, $p<0.01$) (Fig. 4b, Lane: H). Thrombin, known to cause an increase in MLC phosphorylation through RhoA-Rho kinase axis (23), induced an increase in MLC phosphorylation by 146.1±24.3% (n=3, $p<0.05$) over control (Fig. 4b, Lane: T). The densitometric analysis of MLC phosphorylation gels are summarized in Fig. 4c.

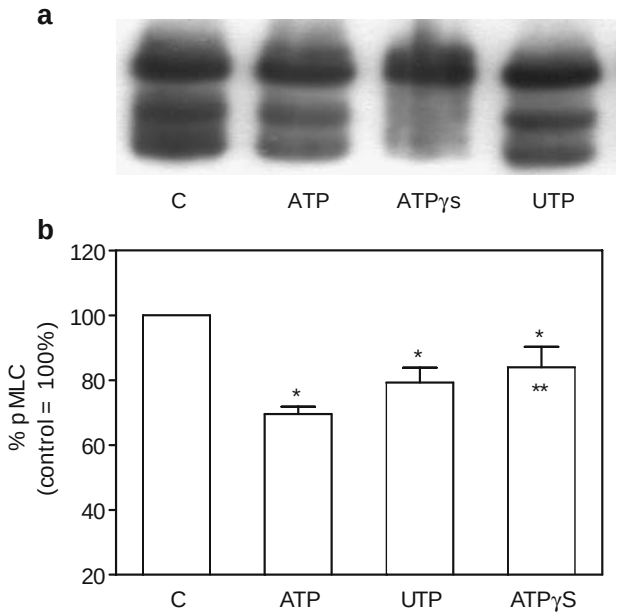

Fig. 6. MLC dephosphorylation induced by P2Y2 agonists. Cells were exposed to 100 μm ATP, UTP or ATPγS for 18 min before MLC phosphorylation assay was performed. **a** A typical urea-glycerol gel showing MLC dephosphorylation induced by all the three P2Y2 receptor agonists. **b** A summary plot of the densitometric analysis of the results. *Indicates significant difference from the control. Notes: C vs. ATP: $p<0.001$; C vs. UTP: $p<0.01$; C vs. ATPγs: $p<0.05$. ** Indicates significant difference ATP vs. ATPγs ($p<0.05$).

Expression of G protein-coupled Purinergic Receptors

Extracellular ATP elevates the intracellular Ca^{2+} level through P2Y2 receptors coupled to $G\alpha_q$ G proteins. However, it has been found to induce MLC dephosphorylation in endothelial cells (27,28) partly through adenosine, which is formed by hydrolysis of ATP. In certain cell types, adenosine is known to activate A2B receptors coupled to $G_{\alpha s}$ G-proteins (28). CD39, the membrane-bound ecto-ATPase, catalyzes hydrolysis of ATP to ADP as well as ADP to AMP (36,37). AMP is degraded to adenosine by 5′-nucleotidase CD73 (38). To investigate the potential effects of ATP in BCEC on MLC phosphorylation, we first examined expression of P2Y and A2B receptors. The RT-PCR results show positive bands for both P2Y2 (274 bp) and A2B (438 bp) receptors, in Fig. 5a and b, respectively. Expression levels of P2Y1 (561 bp), and A2A (789 bp) were not detectable. Transcripts for CD39 (870 bp) and CD73 (1,317 bp) were also found (Fig. 5c).

P2Y2 Agonists Induce MLC Dephosphorylation

Cells were challenged with ATP and its P2Y2 analogues, UTP and ATPγS (100 μm for 18 min). All of these P2Y2 agonists induced MLC dephosphorylation: 30.46% for ATP ($n=7$, $p<0.001$), 20.76% for UTP ($n=4$, $p<0.01$), and 16.03% for ATPγS ($n=4$, $p<0.05$). A typical urea-glycerol gel is shown in Fig. 6a and the densitometric analysis of similar experiments is summarized in Fig. 6b.

Histamine-stimulated MLC Phosphorylation is Opposed by ATP

As shown in Fig. 7, MLC phosphorylation induced by histamine (100 μm, 2 min; 123.6±3.6%; $n=7$, $p<0.01$) is significantly reduced (84.03±5.4%; $n=7$, $p<0.001$) by pretreatment with ATP (100 μm, 18 min).

Effect of Histamine on Organization of Cortical Actin

As shown in Fig. 8a, phalloidin staining demonstrates a cortical band of actin cytoskeleton in BCEC under resting conditions. This organization is disrupted by exposure to histamine (100 μm, 2 min) (Fig. 8b). Pre-treatment with ATP (100 μm, 18 min) reduced the histamine effect (Fig. 8d). No significant change was noticed with ATP alone (Fig. 8c).

Effect of Histamine on Barrier Integrity

To examine the effect of MLC phosphorylation on the epithelial barrier integrity, HRP (44 kDa) permeability across monolayers on Transwell™ porous filters was measured. Fig. 9a shows the accumulation of HRP in the

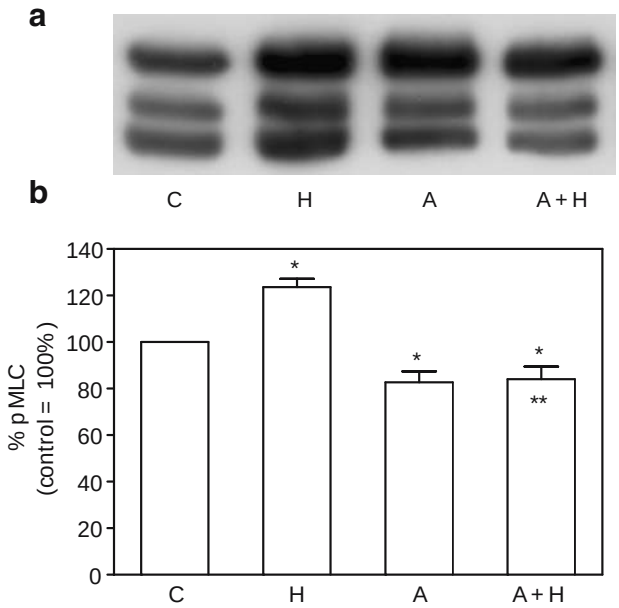

Fig. 7. ATP opposed histamine-induced MLC phosphorylation. Cells were serum-starved for 16–18 h and then subjected to pre-exposure to ATP (100 μm, 18 min) before histamine (100 μm, 2 min) treatment. **a** A typical urea-glycerol gel showing histamine-induced MLC phosphorylation (Lane: H) which is suppressed by co-treatment with ATP (Lane: H + A). **b** A summary plot of the densitometric analysis of the results. Notes: *H*: histamine; *A*: ATP. *Indicates significant difference from the control. C vs. H: $p<0.01$; C vs. ATP: $p<0.05$. **Indicates significant difference H vs. H + ATP ($p<0.001$).

basolateral chamber in untreated cells and in those treated with histamine (100 μm, 2 min) or after pretreatment with ATP (100 μm, 2 min). The enhanced accumulation in the presence of histamine is suppressed by ATP (n=5, p<0.001). Fig. 9b shows similar experiments with the level of HRP measured at 45 min after treatment with various drugs. Consistent with inhibition of histamine-induced MLC phosphorylation, PKC inhibitor chelerythrine also inhibited enhanced HRP permeability in response to histamine.

DISCUSSION

MLC phosphorylation, which triggers increased contractility of the actin cytoskeleton, is a point of convergence of many signal transduction pathways that affect the function of tight junctions (20,21). In the present study, we have investigated MLC phosphorylation and its significance in the regulation of barrier integrity in corneal epithelial cells. The major findings suggest a disruption of the epithelial barrier integrity concomitant with MLC phosphorylation in response to histamine. In consistence, the extracellular ATP, which opposed MLC phosphorylation by histamine, prevented the histamine-induced effect on the barrier integrity. These results suggest a significant effect of increased actin contractility on the regulation of barrier integrity in the corneal epithelium.

We first identified expression of MLCK and RhoA, the two key regulators of MLC phosphorylation at the mRNA level (Fig. 1a). In contrast with the corneal endothelial cells, which were found to express both EC- and SM-isoforms of MLCK (16), cultured BCEC only expresses the EC-MLCK isoform. This was also found in fresh corneal epithelial cells

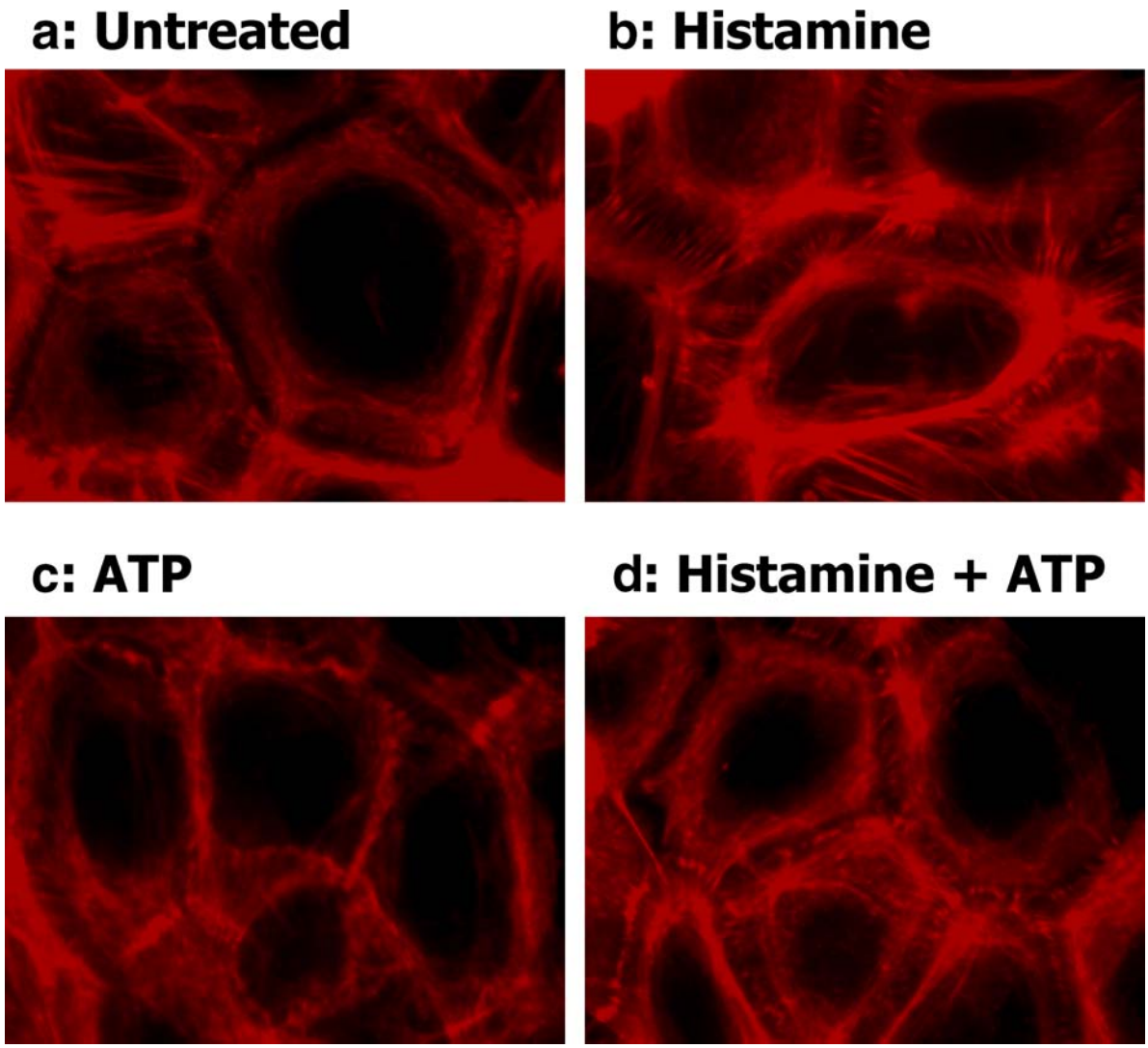

Fig. 8. Effect of histamine on the cortical actin. Cells grown on coverslips were labeled with Texas red phalloidin after exposure to histamine (100 μm, 2 min), ATP (100 μm, 18 min) or both. **a** Actin cytoskeleton forms a dense cortical band along the periphery of untreated cells. **b** Histamine causes actomyosin contraction and disruption of the cortical actin assembly. **c** No significant change was noticed with ATP alone. **d** ATP overcomes the changes in the cortical actin induced by histamine.

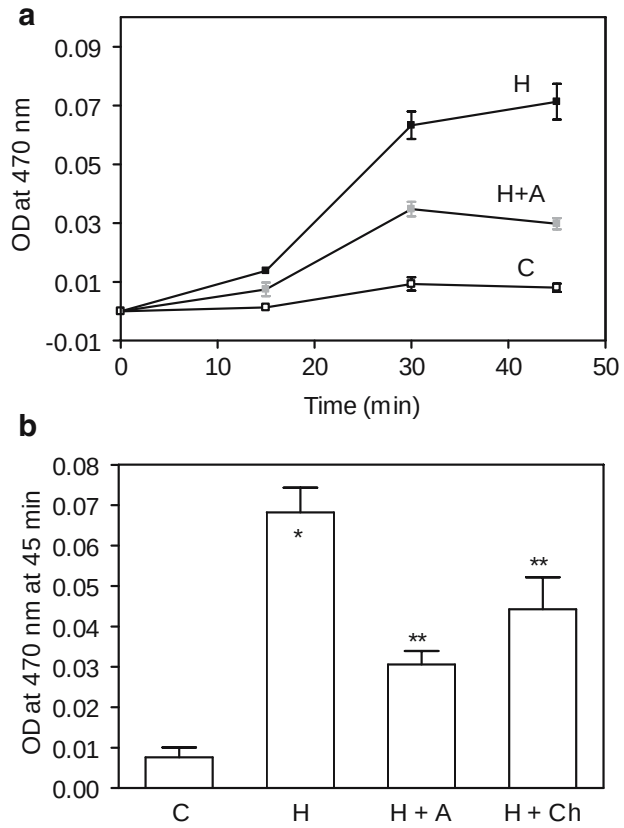

Fig. 9. Histamine-induced disruption of the barrier integrity. BCEC monolayers grown on porous filters were exposed to different drugs and HRP (44 kDa) flux across the monolayers was assessed by measuring peroxidase activity of the basolateral solution. **a** Time-course of HRP accumulation in the basolateral chamber after drug treatment. Each data point represents an average of four independent experiments. Note that exposure to histamine (100 μm, 2 min) resulted in a large accumulation of HRP compared to those in the presence of ATP (100 μm, 10 min) and in untreated cells. **b** Similar experiments but the basolateral solution was only sampled at 45 min. Notes: *C*: Control; *H*: Histamine; *A*: ATP; *Ch*: chelerythrine. * Indicates significant difference C vs. H ($p<0.001$). ** Indicates significant difference H vs. H + A ($p<0.001$) and H vs. H + Ch ($p<0.05$).

(Fig. 1b). The major difference between EC-MLCK and SM-MLCK is the extended N-terminal sequence, which contains multiple regulatory regions for a variety of protein kinases including PKA (31).

The histamine-induced MLC phosphorylation observed in our experiments (Fig. 3) is in agreement with findings in the vascular (23) and corneal (24) endothelial cells. The phosphorylation can be attributed to activation through $G_{\alpha q/11}$ -coupled H1 receptors in BCEC (Fig. 2), which leads to Ca^{2+} mobilization and activation of Ca^{2+}/calmodulin-sensitive MLCK (Fig. 10). In addition, PKC activation secondary to H1 receptors is also involved. PKC phosphorylates CPI-17 (PKC-potentiated inhibitory protein of 17 kDa), which is known to inhibit PP1Cδ (the catalytic subunit of MLCP) (39,40) (Fig. 10). Our observation that the histamine effects are blocked by the PKC inhibitor chelerythrine (Figs. 3 and 9b) suggests a significant role for PKC in the regulation of barrier integrity in BCEC. When compared with cultured cells, fresh BCEC showed a higher degree of MLC phosphorylation in response to histamine. The expression level of the H1 receptor in the fresh cells appears comparable to that in the cultured cells (Figs. 2a and 4a). However, serum starvation in the latter could have down-regulated the responsiveness of the H1 receptor (41).

Although extracellular ATP induces Ca^{2+} mobilization, dephosphorylation has been reported upon exposure to ATP in vascular and corneal endothelial cells (27,42). Similarly, MLC dephosphorylation was found in BCEC upon ATP exposure (Fig. 6). The effect can be attributed partially to the activation of P2Y2 receptors since UTP also elicited MLC dephosphorylation (Fig. 6). Compared with ATP and UTP, ATPγS induced a lesser degree of MLC dephosphorylation (Fig. 6). Since ATPγS is non-hydrolysable and its action is restricted to P2Y2 receptor, our observations imply an additional contribution from byproducts of ATP hydrolysis to the dephosphorylation (Fig. 10). In support of this claim, ecto-ATPase (CD39) and ecto-5′-nucleotidase (CD73) were found to be expressed in BCEC (Fig. 5c) along with adenosine-sensitive A2B receptors (Fig. 5b). Activation of $G_{\alpha s}$ protein-coupled A2B leads to cAMP elevation. Hence, exposure to ATP could result in elevated cAMP in BCEC. By inhibiting RhoA (43), cAMP can stimulate the activity of MLCP which favors MLC dephosphorylation (Fig. 10). As a physiological mediator, ATP is released from injured (44) cells, mechanically stimulated cells (45), and nerve endings (44). Its antagonistic effects towards histamine imply a protective role for the nucleotide at the corneal surface.

To our knowledge, MLC phosphorylation and its association with the barrier integrity have not been reported in corneal epithelial cells. Our observations demonstrate that an increase in MLC phosphorylation results in a disruption of the cortical actin (Fig. 8) and barrier integrity (Fig. 9) in BCEC. These are in agreement with findings in other epithelial and endothelial cell types, which are attributed to a breakdown of the tethering forces required for interactions of the trans-membrane proteins at the tight junctions. The loss of the tethering forces is due to generation of a centripetal force secondary to actomyosin contraction of the PAMR (12–14,46). Thus, a restoration of actin contractility to the levels found in resting conditions can be expected to restore the loss of barrier integrity. As shown in the present study, when the histamine-induced MLC phosphorylation is reduced by chelerythrine (Fig. 3) or ATP (Fig. 7), the breakdown of the barrier integrity is also reduced (Fig. 10).

In summary, we have shown that histamine induces MLC phosphorylation concomitant with a loss of barrier integrity in BCEC, presumably through both Ca^{2+}- and PKC-dependent mechanisms. The histamine effects were opposed by extracellular ATP, which induces MLC dephosphorylation. These findings suggest a regulatory role of MLC-mediated actin contractility in the barrier function of the corneal epithelium.

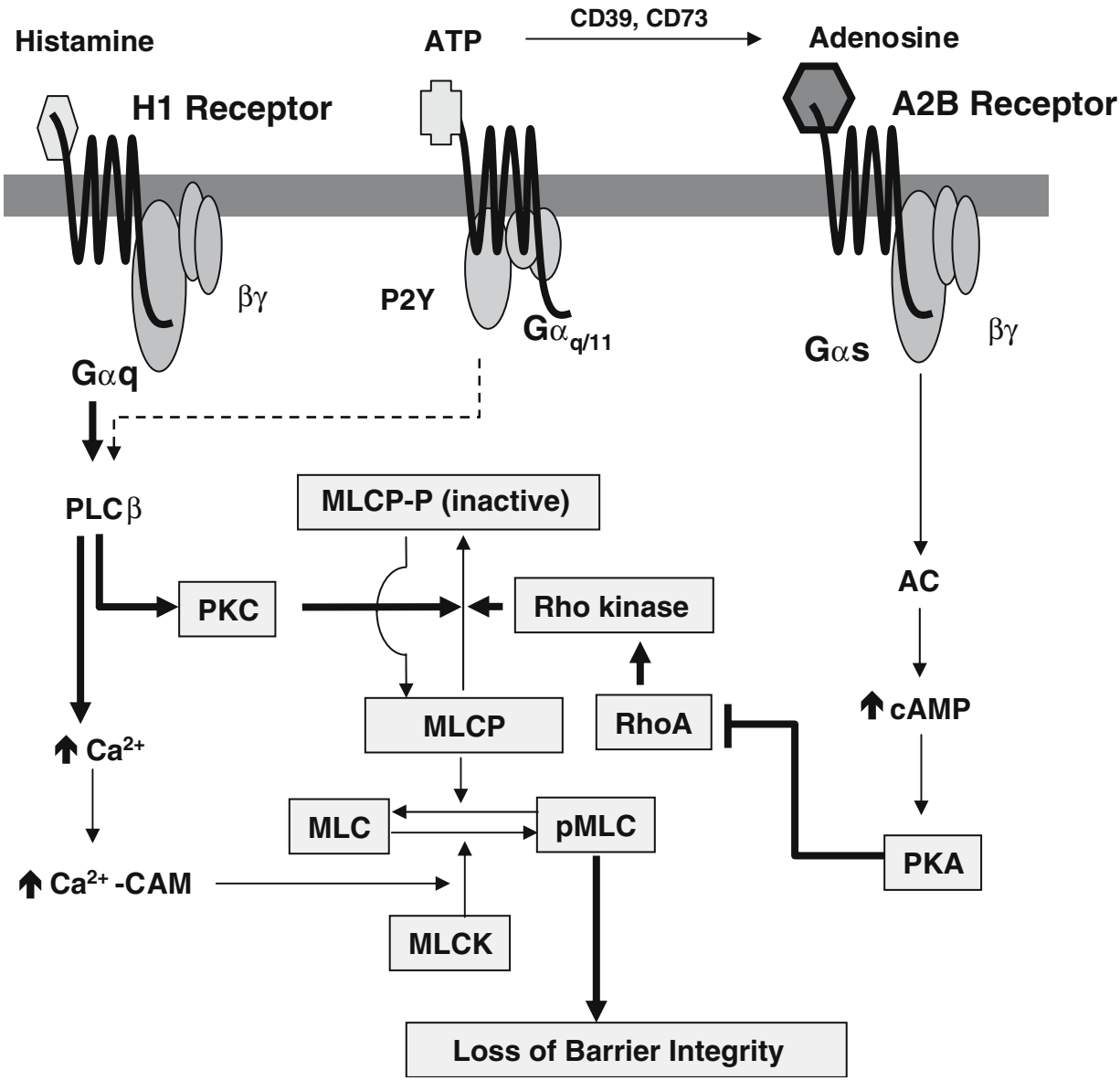

Fig. 10. Schematic showing the cell signaling involved in histamine-induced MLC phosphorylation. Histamine activates H1 receptors, leading to Ca^{2+} mobilization and activation of PKC. Ca^{2+} activates MLCK and drives MLC phosphorylation. On the other hand, PKC inactivates MLCP and thereby enhances MLC phosphorylation. Elevated cAMP activates PKA which, in turn, inhibits RhoA activation. This leads to inhibition of Rho kinase-mediated inactivation of MLCP. Extracellular ATP is converted to adenosine through catalytic activity of ecto-ATPases (CD39 and CD73). Adenosine activates A2B receptors leading to an increase in cAMP.

ACKNOWLEDGEMENTS

Supported by VISTAKON Research Grant, American Optometric Foundation, 2004 (SPS) and NEI 14415 (SPS).

REFERENCES

1. B. J. McLaughlin, R. B. Caldwell, Y. Sasaki, and T. O. Wood. Freeze-fracture quantitative comparison of rabbit corneal epithelial and endothelial membranes. *Curr. Eye Res.* **4**:951–961 (1985).
2. Y. Wang, M. Chen, and J. M. Wolosin. ZO-1 in corneal epithelium; stratal distribution and synthesis induction by outer cell removal. *Exp. Eye Res.* **57**:283–292 (1993).
3. J. M. Diamond. Twenty-first Bowditch lecture. The epithelial junction: bridge, gate, and fence. *Physiologist* **20**:10–18 (1977).
4. B. Gumbiner. Structure, biochemistry, and assembly of epithelial tight junctions. *Am. J. Physiol.* **253**:C749–C758 (1987).
5. M. A. Behzadian, X. L. Wang, L. J. Windsor, N. Ghaly, and R. B. Caldwell. TGF-beta increases retinal endothelial cell permeability by increasing MMP-9: possible role of glial cells in endothelial barrier function. *Investig. Ophthalmol. Vis. Sci.* **42**:853–859 (2001).
6. F. Hollande, E. M. Blanc, J. P. Bali, R. H. Whitehead, A. Pelegrin, G. S. Baldwin, and A. Choquet. HGF regulates tight

junctions in new nontumorigenic gastric epithelial cell line. *Am. J. Physiol.: Gasterointest. Liver Physiol.* **280**:G910–G921 (2001).
7. S. V. Walsh, A. M. Hopkins, and A. Nusrat. Modulation of tight junction structure and function by cytokines. *Adv. Drug Deliv. Rev.* **41**:303–313 (2000).
8. B. P. McNamara, A. Koutsouris, C. B. O'Connell, J. P. Nougayrede, M. S. Donnenberg, and G. Hecht. Translocated EspF protein from enteropathogenic Escherichia coli disrupts host intestinal barrier function. *J. Clin. Invest.* **107**:621–629 (2001).
9. X. Yi, Y. Wang, and F. S. Yu. Corneal epithelial tight junctions and their response to lipopolysaccharide challenge. *Investig. Ophthalmol. Vis. Sci.* **41**:4093–4100 (2000).
10. M. Itoh, M. Furuse, K. Morita, K. Kubota, M. Saitou, and S. Tsukita. Direct binding of three tight junction-associated MAGUKs, ZO-1, ZO-2, and ZO-3, with the COOH termini of claudins. *J. Cell Biol.* **147**:1351–1363 (1999).
11. A. Nusrat, J. R. Turner, and J. L. Madara. Molecular physiology and pathophysiology of tight junctions. IV. Regulation of tight junctions by extracellular stimuli: nutrients, cytokines, and immune cells. *Am. J. Physiol.: Gasterointest. Liver Physiol.* **279**:G851–G857 (2000).
12. J. G. Garcia, H. W. Davis, and C. E. Patterson. Regulation of endothelial cell gap formation and barrier dysfunction: role of myosin light chain phosphorylation. *J. Cell. Physiol.* **163**:510–522 (1995).
13. J. R. Turner. 'Putting the squeeze' on the tight junction: understanding cytoskeletal regulation. *Semin. Cell Dev. Biol.* **11**:301–308 (2000).
14. S. M. Dudekand and J. G. Garcia. Cytoskeletal regulation of pulmonary vascular permeability. *J. Appl. Physiol.* **91**:1487–1500 (2001).
15. H. Lumand and A. B. Malik. Regulation of vascular endothelial barrier function. *Am. J. Physiol.* **267**:L223–L241 (1994).
16. M. Satpathy, P. Gallagher, M. Lizotte-Waniewski, and S. P. Srinivas. Thrombin-induced phosphorylation of the regulatory light chain of myosin II in cultured bovine corneal endothelial cells. *Exp. Eye Res.* **79**:477–486 (2004).
17. R. Yuhan, A. Koutsouris, S. D. Savkovic, and G. Hecht. Enteropathogenic Escherichia coli-induced myosin light chain phosphorylation alters intestinal epithelial permeability. *Gastroenterology* **113**:1873–1882 (1997).
18. Y. Zolotarevsky, G. Hecht, A. Koutsouris, D. E. Gonzalez, C. Quan, J. Tom, R. J. Mrsny, and J. R. Turner. A membrane-permeant peptide that inhibits MLC kinase restores barrier function in in vitro models of intestinal disease.[erratum appears in Gastroenterology 2002 Oct;123(4):1412]. *Gastroenterology* **123**:163–172 (2002).
19. L. Shen, E. D. Black, E. D. Witkowski, W. I. Lencer, V. Guerriero, E. E. Schneeberger, and J. R. Turner. Myosin light chain phosphorylation regulates barrier function by remodeling tight junction structure. *J. Cell Sci.* **119**:2095–2106 (2006).
20. K. E. Kammand and J. T. Stull. Dedicated myosin light chain kinases with diverse cellular functions. *J. Biol. Chem.* **276**:4527–4530 (2001).
21. A. P. Somlyo and A. V. Somlyo. Ca2+ sensitivity of smooth muscle and nonmuscle myosin II: modulated by G proteins, kinases, and myosin phosphatase. *Physiol. Rev.* **83**:1325–1358 (2003).
22. A. B. Moy, J. Van Engelenhoven, J. Bodmer, J. Kamath, C. Keese, I. Giaever, S. Shasby, and D. M. Shasby. Histamine and thrombin modulate endothelial focal adhesion through centripetal and centrifugal forces. *J. Clin. Invest.* **97**:1020–1027 (1996).
23. G. P. Van Nieuw Amerongenvan, R. Draijer, M. A. Vermeer, and V. W. Van Hinsberghvan. Transient and prolonged increase in endothelial permeability induced by histamine and thrombin: role of protein kinases, calcium, and RhoA. *Circ. Res.* **83**:1115–1123 (1998).
24. S. P. Srinivas, M. Satpathy, Y. Guo, and V. Anandan. Histamine-induced phosphorylation of the regulatory light chain of myosin II disrupts the barrier integrity of corneal endothelial cells. *Investig. Ophthalmol. Vis. Sci.* **47**:4011–4018 (2006).
25. A. Leonardi. The central role of conjunctival mast cells in the pathogenesis of ocular allergy. *Curr. Allergy Asthma Rep.* **2**:325–331 (2002).
26. L. Bieloryand and S. Ghafoor. Histamine receptors and the conjunctiva. *Curr. Opin. Allergy Clin. Immunol.* **5**:437–440 (2005).
27. T. Noll, M. Schafer, U. Schavier-Schmitz, and H. M. Piper. ATP induces dephosphorylation of myosin light chain in endothelial cells. *Am. J. Physiol., Cell Physiol.* **279**:C717–C723 (2000).
28. M. Satpathy, P. Gallagher, Y. Jin, and S. P. Srinivas. Extracellular ATP opposes thrombin-induced myosin light chain phosphorylation and loss of barrier integrity in corneal endothelial cells. *Exp. Eye Res.* **81**:183–192 (2005).
29. S. P. Srinivas, M. Satpathy, P. Gallagher, E. Lariviere, and W. Van Driessche. Adenosine induces dephosphorylation of myosin II regulatory light chain in cultured bovine corneal endothelial cells. *Exp. Eye Res.* **79**:543–551 (2004).
30. A. P. Somlyo and A. V. Somlyo. Signal transduction and regulation in smooth muscle.[erratum appears in Nature 1994 Dec 22–29;372(6508):812]. *Nature* **372**:231–236 (1994).
31. V. Lazarand and J. G. Garcia. A single human myosin light chain kinase gene (MLCK; MYLK). *Genomics* **57**:256–267 (1999).
32. K. Kimura, M. Ito, M. Amano, K. Chihara, Y. Fukata, M. Nakafuku, B. Yamamori, J. Feng, T. Nakano, K. Okawa, A. Iwamatsu, and K. Kaibuchi. Regulation of myosin phosphatase by Rho and Rho-associated kinase (Rho-kinase)[see comment]. *Science* **273**:245–248 (1996).
33. K. M. Crawford, D. K. MacCallum, and S. A. Ernst. Histamine H1 receptor-mediated Ca2+ signaling in cultured bovine corneal endothelial cells. *Investig. Ophthalmol. Vis. Sci.* **33**:3041–3049 (1992).
34. K. M. Crawford, D. K. MacCallum, and S. A. Ernst. Agonist-induced Ca2+ mobilization in cultured bovine and human corneal endothelial cells. *Curr. Eye Res.* **12**:303–311 (1993).
35. N. A. Sharif, T. K. Wiernas, W. E. Howe, B. W. Griffin, E. A. Offord, and A. M. Pfeifer. Human corneal epithelial cell functional responses to inflammatory agents and their antagonists. *Investig. Ophthalmol. Vis. Sci.* **39**:2562–2571 (1998).
36. A. Kittel, E. Kaczmarek, J. Sevigny, K. Lengyel, E. Csizmadia, and S. C. Robson. CD39 as a caveolar-associated ectonucleotidase. *Biochem. Biophys. Res. Commun.* **262**:596–599 (1999).
37. A. J. Marcus, M. J. Broekman, J. H. Drosopoulos, N. Islam, D. J. Pinsky, C. Sesti, and R. Levi. Metabolic control of excessive extracellular nucleotide accumulation by CD39/ecto-nucleotidase-1: implications for ischemic vascular diseases. *J. Pharmacol. Exp. Ther.* **305**:9–16 (2003).
38. T. Hashikawa, M. Takedachi, M. Terakura, T. Saho, S. Yamada, L. F. Thompson, Y. Shimabukuro, and S. Murakami. Involvement of CD73 (ecto-5′-nucleotidase) in adenosine generation by human gingival fibroblasts. *J. Dent. Res.* **82**:888–892 (2003).
39. M. Eto, T. Ohmori, M. Suzuki, K. Furuya, and F. Morita. A novel protein phosphatase-1 inhibitory protein potentiated by protein kinase C. Isolation from porcine aorta media and characterization. *J. Biochem.* **118**:1104–1107 (1995).
40. M. Eto, S. Senba, F. Morita, and M. Yazawa. Molecular cloning of a novel phosphorylation-dependent inhibitory protein of protein phosphatase-1 (CPI17) in smooth muscle: its specific localization in smooth muscle. *FEBS Lett.* **410**:356–360 (1997).
41. S. M. Bloemers, S. Verheule, M. P. Peppelenbosch, M. J. Smit, L. G. Tertoolen, and S. Laatde. Sensitization of the histamine H1 receptor by increased ligand affinity. *J. Biol. Chem.* **273**:2249–2255 (1998).
42. T. Noll, H. Holschermann, K. Koprek, D. Gunduz, W. Haberbosch, H. Tillmanns, and H. M. Piper. ATP reduces macromolecule permeability of endothelial monolayers despite increasing [Ca2+]i. *Am. J. Physiol.* **276**:H1892–H1901 (1999).
43. J. Qiao, F. Huang, and H. Lum. PKA inhibits RhoA activation: a protection mechanism against endothelial barrier dysfunction. *Am. J. Physiol., Lung Cell. Mol. Physiol.* **284**:L972–L980 (2003).
44. G. Burnstock. P2 purinoceptors: historical perspective and classification. *Ciba Found. Symp.* **198**:1–28; discussion 29–34 (1996).
45. K. Enomoto, K. Furuya, S. Yamagishi, T. Oka, and T. Maeno. The increase in the intracellular Ca2+ concentration induced by mechanical stimulation is propagated via release of pyrophosphorylated nucleotides in mammary epithelial cells. *Pflugers Arch. Gesamte Physiol. Menschen Tiere* **427**:533–542 (1994).
46. J. R. Turner, B. K. Rill, S. L. Carlson, D. Carnes, R. Kerner, R. J. Mrsny, and J. L. Madara. Physiological regulation of epithelial tight junctions is associated with myosin light-chain phosphorylation. *Am. J. Physiol.* **273**:C1378–C1385 (1997).